

## Formimidoyl Group Transfer from Activated Amidines. Part 1. Hydrolysis of 1-(*N*-*t*-Butylformimidoyl)imidazole and Related Imidazole-containing Formamides

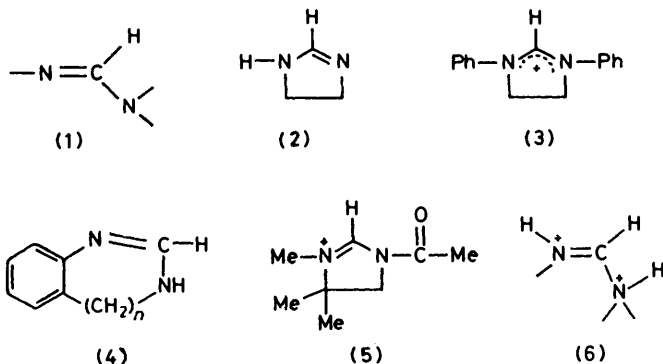
By Anne Chandler, Anthony F. Hegarty,\*† and Margaret T. McCormack, Chemistry Department, University College, Cork, Ireland

The hydrolysis of 1-(*N*-*t*-butylformimidoyl)imidazole (7a) to *t*-butylformamide and imidazole has been examined in the absence of buffer species at 25° in water. The rate of hydrolysis was pH-independent at pH 7–14 and reaction in this region is shown to occur *via* HO<sup>-</sup> attack on the protonated substrate (whose *pK<sub>a</sub>* is 5.0; protonation site, imidazole nitrogen). Alternative mechanisms such as H<sub>2</sub>O attack on the neutral substrate and reaction *via* the zwitterion (15) were eliminated using solvent isotope effect, deuterium labelling, and substituent effects. Below pH 6 acid catalysis of hydrolysis is observed due to H<sub>2</sub>O reaction with the protonated substrate (pH 4–6) and with the diprotonated substrate (pH 0–4); at pH 0, *t*<sub>1/2</sub> for hydrolysis is <10<sup>-2</sup>s. The *N*-arylformamidines (7b) and (7c) react *via* similar acid catalysed pathways but a new reaction (identified as HO<sup>-</sup> attack on the amidine) occurs in base, in preference to the pH independent pathways. *p*-Nitrophenylformamide [formed from (7c)] is itself hydrolysed in basic solution so that complex kinetics result. The *C*-substituted amidines (7e) and (7f) react 10<sup>4</sup>–10<sup>2</sup>-fold more slowly than the corresponding formamidines. Buffer catalysis of the hydrolysis of (7a) by phosphate and amines is complex, the slope of *k<sub>obs</sub>* *versus* [buffer] plots being greater at low than at high buffer concentrations. This is consistent with the formation of a tetrahedral intermediate in the reaction pathway whose formation and breakdown is subject to general acid–base catalysis.

SIMPLE amidines (1) and their cyclic analogues, the imidazolidines (2), have been used as model substrates to study the transfer of a one-carbon unit which occurs in reactions involving tetrahydrofolate co-enzymes.<sup>1</sup> These include the catalysed hydrolysis of 1,3-diphenylimidazolium ion (3) studied by Robinson and Jencks,<sup>2</sup> which was shown to involve solvent addition to the cation giving a tetrahedral intermediate followed by general acid–base catalysed breakdown of the tetrahedral intermediate. This tetrahedral intermediate could be observed<sup>3</sup> in highly alkaline solution and was at the time of the report the first direct observation of such an intermediate at the acyl level of oxidation. More recently, extensive studies have been carried out by Benkovic and his co-workers<sup>1,4</sup> on the mechanisms of

amine as nucleophile, net formyl-group transfer does occur although complex kinetics result since the initial product of overall one-carbon-unit transfer, mimicking control are different. Suitably substituted imidazolium salts such as (5) undergo nucleophilic attack and ring opening with monofunctional reagents such as amines to give ω-amino-amidines. With bifunctional nucleophiles the intermediates undergo further reaction to yield the product of overall one-carbon-unit transfer, mimicking the biochemical process.<sup>5</sup>

Apart from the initial work by DeWolfe,<sup>6,7</sup> there is, however, little data available on the effect of structure on the reactivity of simple acyclic amidines. In particular the possibility of reaction occurring *via* a diprotonated substrate (6) at moderate acidity has not been examined. Part of this problem arises from the very low reactivity shown by simple amidines in aqueous and particularly in acidic solution. We have overcome this reactivity problem by examining the amidine (7) in which one of the nitrogens forms part of an imidazole ring. This has two effects: (a) the amidine group is more highly reactive towards nucleophilic attack because of the involvement of the lone pair of the nitrogen in the imidazole ring (rather than in stabilization of the amidine linkage); (b) protonation can occur at the 'remote' nitrogen of the imidazole function, enhancing the possibility of diprotonation of the amidine at moderate acidities. Such an approach has previously been used successfully with the activation of acylimidazoles as shown by the high reactivity of acylimidazoles and the azolides.<sup>8–10</sup>



folate cofactors including studies of cyclic amidines of type (4) with varying ring size, in order to probe the role of stereoelectronic effects on the breakdown of tetrahedral intermediates. Although the importance of stereoelectronic effects could not be unequivocally proven, it was shown that for (4; *n* = 2) with methoxy-

† Present address: Chemistry Department, University College, Belfield, Dublin 4, Ireland.

### RESULTS AND DISCUSSION

*pH Rate Profile.*—The hydrolysis of 1-(*N*-*t*-butylformimidoyl)imidazole (7a) has been investigated in water at 25° (*μ* 1.0; KCl) as a function of pH. The products formed at all pH values were imidazole and

t-butylformamide (8a). The rate constants obtained are summarised in Figure 1; this shows two regions (pH < 3 and 5–7) where the rate of hydrolysis of (7a) is directly proportional to  $[H^+]$ , and two regions (pH *ca.* 4 and 8–14) where the rate of reaction is pH-independent. The solid line in Figure 1 fits the data closely; the equation of this line is given by equation (1) which

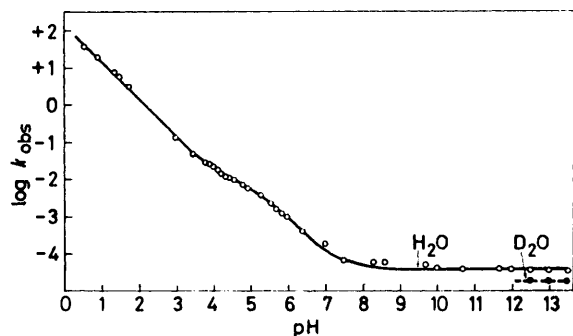


FIGURE 1 Plot of log of first-order rate constants ( $k_{obs}/s^{-1}$ ) for the hydrolysis of 1-(*N*-t-butylformimidoyl)imidazole (7a) against pH in water (open circles) and  $D_2O$  (closed circles) at 25° ( $\mu$  1.0, KCl). The solid line is theoretical [equation (1), with  $k_1/K_{a2}$   $1.78 \times 10^2 s^{-1}$ ;  $k_2$   $7.8 \times 10^{-3} s^{-1}$ ;  $K_{a1}$   $1.0 \times 10^{-5}$ ;  $k_3$   $3.8 \times 10^4 l mol^{-1} s^{-1}$ ]

can be derived from the kinetic Scheme 1, where (9) and (10) are the protonated and diprotonated substrate respectively, and reaction occurs only through (9a) (with  $HO^-$  and with  $H_2O$ ) and (10a) (with  $H_2O$ ), while  $k_1 = 0$ . The values of the constants which fit equation (1) and were used to draw the solid line in Figure 1 are given in the Table.

Although the data are closely correlated by equation (1), the mechanism of hydrolysis that it describes is not

$$k_{obs.} = \frac{k_4 a_H}{a_H + K_{a2}} + \frac{k_2 a_H}{a_H + K_{a1}} + k_3 [HO^-] \cdot \frac{a_H}{K_{a1}} \quad (1)$$

unique and several kinetically equivalent mechanisms are also considered later (and discarded). The pH regions where the three terms in equation (1) are dominant are taken in turn.

(a) *Acidic solution.* At pH < 3, the only term of importance is that containing  $k_4$ , so that reaction is occurring between the diprotonated form of the substrate (10a) and water. At the lowest pH studied there

TABLE

Rate constants for the hydrolysis of formamides <sup>a</sup>

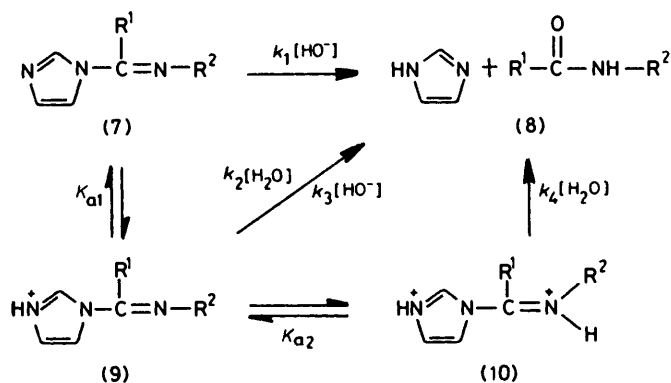
| Substrate | $k_4 K_{a2}^{-1} / s^{-1}$ | $k_2 / s^{-1}$       | $K_{a1}$             | $k_3 / l mol^{-1} s^{-1}$ | $k_1 / l mol^{-1} s^{-1}$ |
|-----------|----------------------------|----------------------|----------------------|---------------------------|---------------------------|
| (7a)      | 178                        | $7.8 \times 10^{-3}$ | $1.0 \times 10^{-5}$ | $3.8 \times 10^4$         |                           |
| (7b)      | 5                          | $1.2 \times 10^{-2}$ | $6.3 \times 10^{-5}$ |                           | $7.9 \times 10^{-2}$      |
| (7c)      | 2                          | $9.9 \times 10^{-3}$ | $7.8 \times 10^{-5}$ |                           | 5.0                       |

<sup>a</sup> See equation (1) and theoretical lines in Figures 1 and 2.

was no indication that the rate of reaction was becoming pH independent [which would show that the substrate was being converted entirely to (10a)] so that  $pK_{a2} < 1$ ; thus neither  $k_4$  nor  $K_{a2}$  could be determined independently. This is not unreasonable since imidoyl halides, where the electron-withdrawing power of the chlorine

should be comparable with that of the protonated imidazole, have  $pK_a$  values < 0.<sup>11</sup>

(b) *Intermediate pH.* At *ca.* pH 4–6 the major reaction is between water and the protonated substrate, *i.e.* the term in equation (1) containing  $k_2$  is dominant. The kinetically equivalent reaction of (10a) with  $HO^-$  can be disregarded since this would have to occur with a rate constant  $> 10^{12} l mol^{-1} s^{-1}$  to explain the observed rate of reaction. The kinetic data implies that the substrate has a  $pK_{a1}$  of 5.0 and this was confirmed spectrophotometrically, a plot of optical density of (7a) at 260 nm against pH giving a  $pK_a$  of 4.98, almost identical with the value which fits the kinetic equation. Because of the high reactivity of the substrate in this pH region the optical density of unchanged (7a) was obtained at the various pH values by extrapolation back to 0%

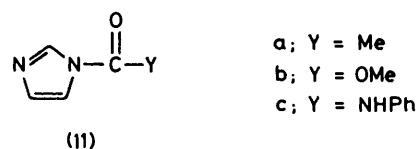


- a;  $R^1 = H, R^2 = CMe_3$   
 b;  $R^1 = H, R^2 = Ph$   
 c;  $R^1 = H, R^2 = p-NO_2C_6H_4$   
 d;  $R^1 = ^2H, R^2 = CMe_3$   
 e;  $R^1 = Me, R^2 = Ph$   
 f;  $R^1 = R^2 = Ph$

SCHEME 1

reacted. The wavelength used to estimate  $pK_{a1}$  was chosen so that the optical density in acid was small; the spectral change in hydrolysis in the more reactive region was therefore quite small, minimising the error in the extrapolations.

The substrate (7a) has two basic sites, N-3 on the imidazole ring and the imino-nitrogen on the chain. Assignment of the  $pK_a$  of 4.98 to protonation of the imidazole group is reasonable when compared with data

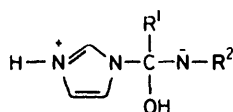


for related materials. Thus acetyl- (11a) and *N*-(methoxycarbonyl)-imidazole (11b) have reported  $pK_a$  values of 3.8 and 3.6, respectively<sup>12,13</sup> while a  $pK_a$  of 4.25 for 1-phenylcarbamoylimidazole (11c) has also been assigned to protonation of the imidazole group.<sup>14</sup> Moreover *N*-aryl substituents on the imino-nitrogen

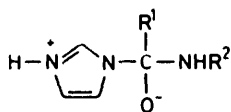
have a relatively small effect on the  $pK_{a1}$  value (see below) making it unlikely that this nitrogen is the first protonation site.

(c) *High pH.* The dominant feature of the pH rate profile of Figure 1 is the pH-independent 'plateau' above pH 8. Several reasonable mechanisms must be considered to explain the behaviour, but we favour hydroxide ion reaction with the protonated substrate (9a), which is kinetically indistinguishable from unimolecular reaction of the neutral substrate (or reaction of the substrate with water) in this pH region. This may involve the formation of a tetrahedral intermediate (12); however Page and Jencks<sup>15</sup> have argued that the analogous intermediate (13) (from the general acid catalysed reaction of acetyl imidazole with hydrazine) is too unstable to exist so that (12) may not be actually formed but loss of neutral imidazole concerted with HO<sup>-</sup> attack.

Such a mechanism is not unreasonable since the  $k_3$  value calculated ( $3.8 \times 10^4 \text{ l mol}^{-1} \text{ s}^{-1}$ ) is within the expected range when compared with the rate of reaction of the protonated substrate with water (*i.e.*  $k_{\text{HO}^-}/k_2$   $4.87 \times 10^6$ ).<sup>16</sup> The product analysis, absence of a



(12)



(13)

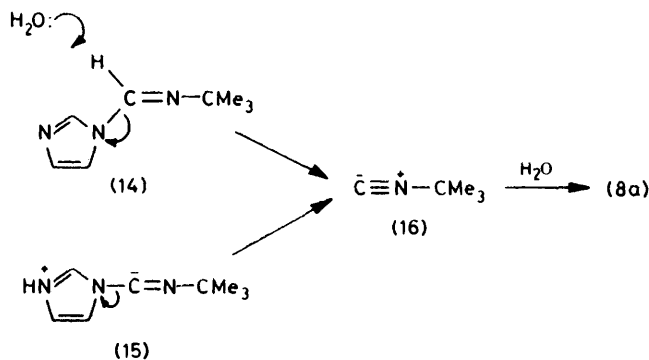
primary deuterium isotope effect, and retention of deuterium in the product (see below) are consistent with this mechanism. A deuterium solvent isotope effect was also measured at high pH (see Figure 1). The observed rate constants were again independent of pH giving  $k_{\text{H}_2\text{O}}/k_{\text{D}_2\text{O}}$  2.0. This value, while being consistent with the proposed mechanism, is not unequivocal, since in reactions in which H<sub>2</sub>O acts as a nucleophile  $k_{\text{H}_2\text{O}}/k_{\text{D}_2\text{O}}$  is typically *ca.* 2.2.<sup>17</sup>

Other kinetically equivalent mechanisms which must be considered are as follows.

(i) Water acting as a nucleophile on the neutral substrate (7a), is unlikely since hydroxide ion, a stronger nucleophile than water, should react  $>10^5$ -fold more rapidly with (7a) (this is a typical value for imines or esters); however even at 1.0M-HO<sup>-</sup>, there is no evidence (see Figure 1) for reaction of the neutral substrate with HO<sup>-</sup>.

(ii) Rate-determining removal of the CH proton as in (14) is broadly the reverse of the reaction used to synthesise (7a) (see Experimental section), and is consistent with the very much lower reactivity (see below) of the C-substituted analogue (7e) which cannot react by this pathway. We therefore examined the reactivity of the deuterio-analogue (7d); this reacted at pH 9–14 at the same rate as the undeuteriated material (7a) which rules out a mechanism depicted in (14) involving partial C-H bond breaking in the transition state. This mechanism also implies the intermediacy of t-butyl

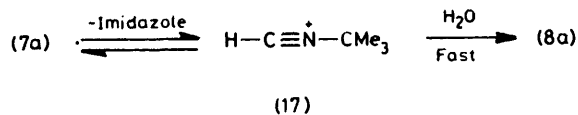
isocyanide (16). We have examined the rate of hydrolysis of (16) at various pH values. The isocyanide was hydrolysed to the amide (8a) only in the presence of acid or base. The rate of hydrolysis in the presence of 1.0M-HCl was  $6.67 \times 10^{-5} \text{ s}^{-1}$  at 60° and  $9.12 \times 10^{-5} \text{ s}^{-1}$  at 60° in the presence of 1.0M-KOH. Since reaction was



proportional to acid or base concentrations, the rate of hydrolysis under neutral conditions at 25° would be immeasurably slow; therefore if (16) was present as a reaction intermediate from (7a) it would have been detectable. We carefully looked for the isocyanide (by extraction into chloroform and analysis by i.r.) and under conditions where control experiments indicated that  $>3\%$  of (16) would have been detected, we found no evidence for its presence. Moreover the deuterium content of t-butylformamide formed from (7d) was the same (*i.e.* 77%) as in the starting amidine whereas hydration of an intermediate (16) would have resulted in loss of deuterium.

(iii) A related mechanism involving pre-equilibrium formation of the zwitterion (15) followed by rate-determining loss of imidazole to give the isocyanide, can also be ruled out on the basis of the products formed and the retention of deuterium in the product.

(iv) Unimolecular ionization to give the nitrilium ion (17) which is trapped by water is also possible. This was ruled out by the absence of a rate depression (mass law effect) in the presence of added imidazole ( $k_{\text{obs.}}$   $2.50 \pm 0.07 \text{ s}^{-1}$  at pH 6.74 with total imidazole concentration in the range 0.01–0.001M). Nitrilium ions



(17) are known to be highly selective and reaction of (17) with imidazole would have re-formed (7a), slowing the overall rate of hydrolysis of (7a).

*Substituent Effects.*—The rates of hydrolysis of 1-(*N*-phenylformimidoyl)- (7b) and 1-(*N*-*p*-nitrophenylformimidoyl)-imidazole (7c) were also studied in water at 25°; the results obtained are summarised in Figure 2. The profiles in acid are broadly similar, with reaction occurring between the mono- and di-protonated species and water. The data were correlated by equation (1)

with the values of the constants given in the Table. As previously mentioned, the relatively small shift in  $K_{a1}$  on changing the substituent on the imino nitrogen from *t*-butyl to phenyl to *p*-nitrophenyl (less than 1.0  $pK_a$  unit) points to the imidazolyl ring as the site of mono-protonation.

At high pH the rate of hydrolysis of compounds (7b and c) are proportional to  $[HO^-]$ , a reaction not observed with (7a). No pH-independent reaction was observed, but this could be present with  $k_{obs.} < 10^{-5} s^{-1}$ . Using the  $k_3/k_2$  value noted above for (7a) a predicted pH independent rate of  $9 \times 10^{-6} s^{-1}$  can be calculated for (7b). The absence of a pH-independent plateau for

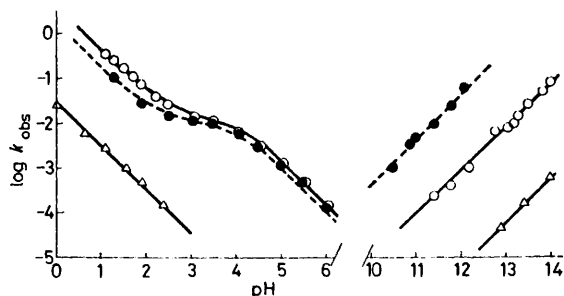
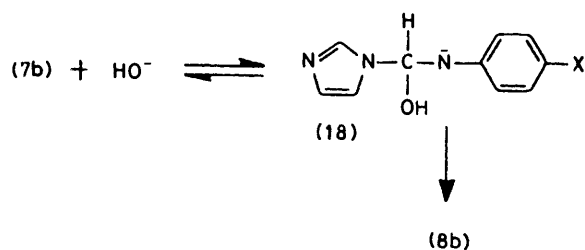


FIGURE 2 Plots of log of the observed rate constants ( $k_{obs.}/s^{-1}$ ) for the hydrolysis of (a) 1-(*N*-*p*-nitrophenylimidoyl)imidazole (7c) (closed circles, broken line); (b) 1-(phenylformimidoyl)imidazole (7b) (open circles, solid line); and (c) 1-(phenylbenzimidoyl)imidazole (7f) (triangles) in water at 25° as a function of pH

(7b) is therefore entirely explicable in terms of the mechanism ( $HO^- +$  protonated substrate) suggested above.

The appearance of  $HO^-$ -catalysed reactions for *N*-aryl substituted amidines is consistent with stabilization of the negative charge generated in the tetrahedral intermediate (18) and, as expected, the substituent X has a large effect on the reaction rate. Thus, assuming a Hammett  $\sigma^-$  value of +1.24 for the *p*- $NO_2$  group, a  $\rho$  value of +1.45 is obtained (from two substituents).<sup>18</sup>

The hydrolysis of (7c) was complicated at pH 10–12.5 by the appearance of a subsequent spectral change which occurred at a comparable rate. This was shown to be due to the hydrolysis of the formamide (8c) which



was also synthesised and examined independently (Scheme 2). Below pH *ca.* 11 the rate of hydrolysis of (8c) is proportional to  $[HO^-]$ ; at high pH hydrolysis becomes independent of pH (Figure 3). The changeover in the order of hydroxide dependence from 1.0 to 0 corresponds to the  $pK_a$  of the formamide (8c) ( $K_{a3}$

$10^{-12}$ ) and this was confirmed by spectrophotometric measurement of the  $pK_a$  of (8c) as 12.08 (25°;  $H_2O$ ;  $\mu$  1.0, KCl;  $\lambda$  385 nm). The most likely mechanism of hydrolysis of the formamide is that shown in Scheme 2; only the formamide (8c) undergoes base-catalysed

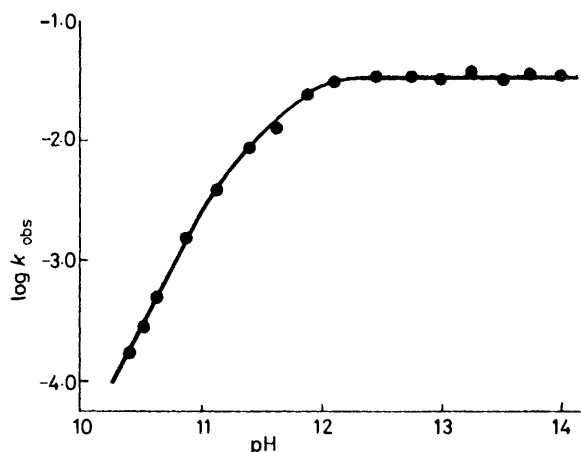
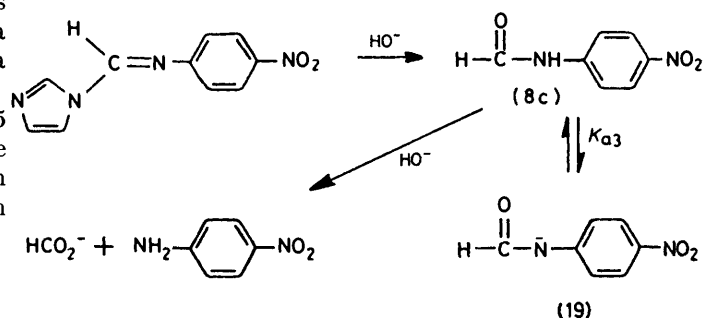


FIGURE 3 Plot of the log of the observed rates of hydrolysis ( $k_{obs.}/s^{-1}$ ) of *p*-nitrophenylformamide in water at 25°. The line is theoretical, using the equation  $k_{obs.} = kK_a/(a_H + K_a)$ , with  $k$   $3.2 \times 10^{-2} s^{-1}$  and  $K_a$   $10^{-12}$

hydrolysis whereas the conjugate base (17), formed at high pH, is unreactive.

The rates of hydrolysis of the amidine (7c) was then corrected for the subsequent hydrolysis of (8c) by taking measurements at isobestic points for the hydrolysis of the latter; since (8c) had its  $pK_a$  in the pH range under study, an isobestic point had to be determined at each pH.

*C*-Substituted Amidines.—Large rate decreases were observed when the C-H of the formamidines were



SCHEME 2

replaced by a Ph or Me group [(7e and f)]. The results for (7f) are recorded in Figure 2, together with the data for the *N*-arylformamides. The *C*-methyl analogue (7e) reacted even more slowly with observed rates of  $1.42 \times 10^{-4}$  and  $9.5 \times 10^{-5} s^{-1}$  at pH 0 and 14, respectively, at 60°. A repetitive scan of the u.v. spectrum of (7f) at pH 7 and 60° showed no detectable reaction over 24 h. The large rate decreases ( $10^2$ – $10^4$ -fold) observed might suggest a special mechanism for the formamidine (involving for example, C-H bond scission) but this possibility was eliminated by various experiments

using the deuteriated formamidine (7d). Both amidines (7e and f) show acid- and base-catalysed hydrolysis; acid-catalysed hydrolysis at pH close to zero must indicate that the diprotonated amidine (10e or f) is the reactive species. The lack of reactivity shown by these C-substituted amidines can therefore be attributed to greater stabilization of the dications, which consequently undergo water attack less rapidly than (10b). This is consistent with recent estimates of the destabilization of carbocation species by a hydrogen (relative to a CH<sub>3</sub> or Ph group) attached directly to carbon.<sup>19</sup>

**Catalysis by Buffer Species.**—(a) *Phosphate buffers.* The catalysis of the conversion of 1-(N-t-butylformimidoyl)imidazole (7a) to (8a) was also examined in the

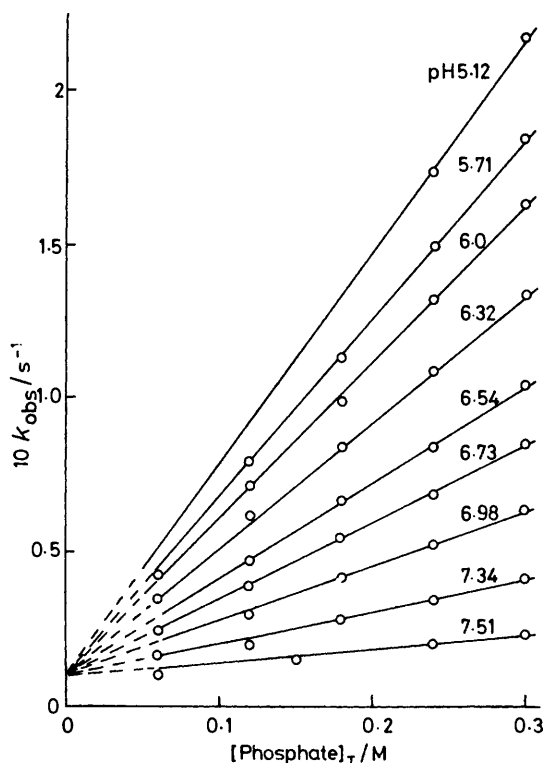


FIGURE 4 Observed rates of hydrolysis of (7a) at 25° ( $\mu$  1.0) as a function of total phosphate buffer concentration and pH. These represent 'high buffer concentrations' (see text) and extrapolate back to  $k_{\text{obs.}} 7.8 \times 10^{-3} \text{ s}^{-1}$  at [buffer] 0

presence of various buffers and showed complex behaviour. Marked buffer catalysis was observed in the presence of phosphate buffers and plots of the observed rate constants *versus* total concentration (*i.e.*  $[\text{H}_2\text{PO}_4^-] + [\text{HPO}_4^{2-}]$ ) were linear at constant pH, but the slopes were largest at lower pH (where the concentration of the acid species,  $\text{H}_2\text{PO}_4^-$ , was largest, see Figure 4). That only general acid catalysis was being observed was confirmed by a linear plot of  $k_{\text{obs.}}$  against  $[\text{H}_2\text{PO}_4^-]$  with data from several pH values. However it will be noted that the value of  $k_0$  (obtained by extrapolation in Figure 4 of  $k_{\text{obs.}}$  to zero buffer concentration) was up to 10-fold greater than the actual value measured (using the pH-stat-spectrophotometer assembly) in the absence of

added buffer at the same pH. Moreover all the lines in Figure 4 extrapolate to a single point ( $k_0 7.8 \times 10^{-3} \text{ s}^{-1}$ ), which is independent of the pH at which the measurement is made.

We have therefore examined buffer catalysis at low phosphate buffer concentrations and confirm that the

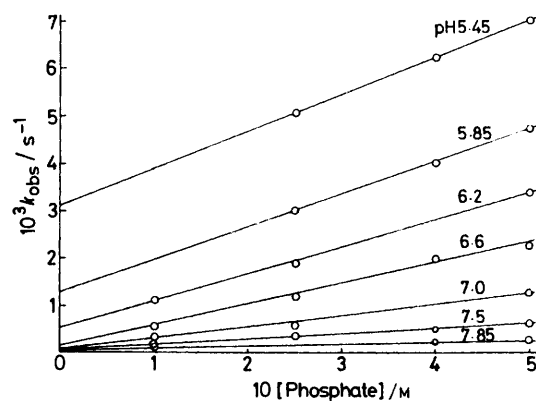


FIGURE 5 Plots of observed rates of hydrolysis of (7a) at 25° ( $\mu$  1.0) as a function of (low) phosphate buffer concentration. Note that the slopes are greater than those of Figure 4 (at the same pH) and that the intercept is variable and corresponds to the 'water rate' (Figure 1)

$k_{\text{obs.}}$  values obtained under these conditions fall *below* the extrapolated lines obtained at high phosphate concentration. Total phosphate buffer concentrations in the range  $1.0\text{--}5.0 \times 10^{-3} \text{ M}$  were used and since phosphate has little buffering capacity in this range, pH was maintained constant by the pH-stat. The results obtained (Figure 5) clearly show that  $k_{\text{obs.}}$  was a linear function of buffer concentration and that general acid catalysis was again observed. This is shown in Figure 6 where the slopes from Figure 5 are plotted against pH; these describe a simple titration curve about the  $pK_a$  for  $\text{H}_2\text{PO}_4^-$ . In this case, however, the extrapolated value

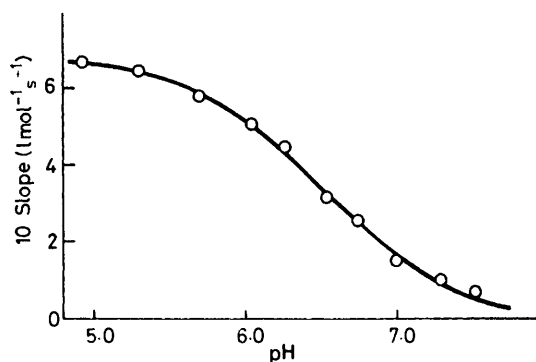


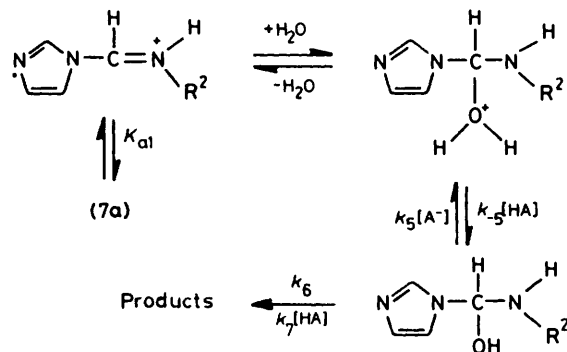
FIGURE 6 Plot of the slopes of the buffer dilution plots of Figure 5 (obtained at low buffer concentration) against pH, which shows that the acidic species ( $\text{HPO}_4^-$ ) is the apparent catalytic species

(at [buffer] 0) varied with pH and was identical with the value obtained in the absence of buffer species.

These results imply that there is a changeover in rate-determining step as the buffer concentration is changed and thus the presence of an intermediate. A kinetic

scheme consistent with this is shown (Scheme 3) where HA is a general acid catalyst (of acidity  $K_{a3}$ ).

At  $\text{pH} > \text{p}K_{a1}$ , the observed rate of reaction is given by equation (2). At high concentrations of [HA],



$k_{-5}[\text{HA}] > k_6 + k_7[\text{HA}]$  so that  $k_{\text{obs}}$  reduces to equation (3); this predicts that a plot of  $k_{\text{obs}}$  against [HA] will be

$$k_{\text{obs}} = \frac{(k_6[\text{HA}] + k_7[\text{HA}]^2)k_5K_{a3}/K_{a1}}{(k_{-5} + k_7)[\text{HA}] + k_5} \quad (2)$$

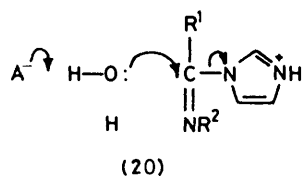
$$k_{\text{obs}} = \frac{k_5K_{a3}}{k_{-5}K_{a1}} \cdot k_6 + \frac{k_5}{k_{-5}} \cdot \frac{K_{a3}}{K_{a1}} \cdot k_7[\text{HA}] \quad (3)$$

linear with intercept  $k_5K_{a3}k_6/k_{-5}K_{a1}$  (as observed, see Figure 4). At low [HA],  $k_6 > k_7[\text{HA}]$  and  $k_5 > k_{-5}[\text{HA}] + k_7[\text{HA}]$ , so that equation (2) reduces to equation (4). This requires a linear dependence of the observed rate on [HA], but without an intercept at [HA] 0 (as observed, see Figure 5).

$$k_{\text{obs}} = k_5K_{a3}[\text{HA}]/K_{a1} \quad (4)$$

Interestingly the value of  $k_{\text{obs}}$  obtained by extrapolation to [HA] 0 (from  $k_{\text{obs}}$  values measured at high [HA], see Figure 4) is  $7.8 \times 10^{-3} \text{ s}^{-1}$ , which is the same as the  $k_2$  value obtained (see Figure 1 and Table) for reaction of the protonated substrate with water. This implies that the same step, *viz.* breakdown of the intermediate,  $k_6$ , is rate determining.

General acid catalysis of hydrolysis of the formamidine could, by analogy with aminolysis of acetyl imidazole, involve rate-determining general base catalysis of water attack on the protonated substrate (20); in fact the



Brønsted  $\alpha$  value of 0.76 (see below) is almost the same as that reported (0.72). However this would lead to an 'intermediate' (12) which (we have commented above) is unlikely to exist. If reaction (20) is concerted (imidazole leaves as the C-O bond is formed) then the biphasic behaviour of phosphate buffers would not be apparent. However Scheme 3 presents just one of several kinetically equivalent possibilities which give

rise to an equation of the format of (2); since attempts to synthesise the *N*-methylimidazolium derivative of (7a) (as a model substrate with a 'fixed' proton position) were unsuccessful, we are unable to distinguish between these.

(b) *Amine buffers.* The 'biphasic' behaviour noted with catalysis by phosphate monoanion is not limited to this general acid (which is a potential bifunctional catalyst) but was also observed with the conjugate acids of amines with  $\text{p}K_a$  values in the same region. For example, with ethyl glycinate the changeover in rate-determining step occurred at *ca.*  $10^{-1}\text{M}$ -buffer at  $\text{pH}$  7.5. With more basic amines (which are weaker acids) linear  $k_{\text{obs}}$  versus [HA] plots were noted, *i.e.* the changeover was not observed up to  $1\text{M}$ -buffer. These results are summarised in terms of the Brønsted plot of Figure 7 which shows the relationship between  $\log k_{\text{HT}}$

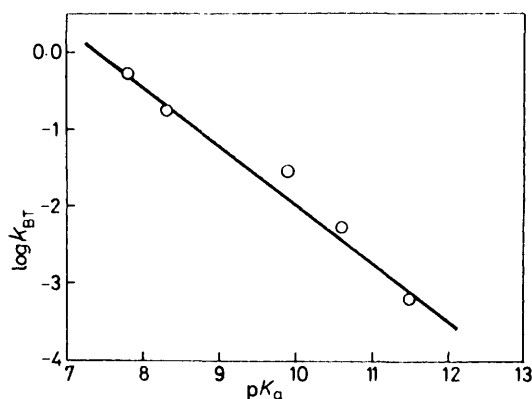


FIGURE 7 Brønsted plot of the second-order rate constants for general acid catalysis hydrolysis of (7a) (data from low amine concentrations; slope  $-0.76$ )

and the  $\text{p}K_a$  of the conjugate acid of the amine; the slope (or Brønsted  $\alpha$  value) is 0.76.

(c) *Catalysis of hydrolysis of (7b).* Buffer catalysis was also shown by the other formamidines studied. The results are summarised for (7b) by the plots of the observed rate of hydrolysis as a function of phosphate buffer concentration at various  $\text{pH}$  values in Figure 8. The plots are of the same type as those obtained for (7a) except that the 'break' or changeover in rate-determining step occurs at higher total phosphate buffer concentration (*ca.*  $0.5\text{M}$ ). The  $k_{\text{obs}}$  versus total buffer plots are strictly linear at low buffer concentration (as shown on an expanded scale) and on extrapolation to zero buffer concentration give rate constants which are identical with those obtained in the absence of buffer species. Extrapolation of the observed rate constants at high buffer concentration (see Figure 8) go through a single point which is independent of  $\text{pH}$ ; this observed rate at [buffer] 0 is  $0.98 \times 10^{-2} \text{ s}^{-1}$ , close to the value of  $k_2$  used ( $1.2 \times 10^{-2} \text{ s}^{-1}$ ) for the reaction of the protonated substrate with water (Figure 2). It is clear therefore that the biphasic behaviour (which is not limited to phosphate buffers) is also shown by other imidazole-containing formamidines.

In conclusion, the incorporation of the imidazole moiety in the formamidine group greatly enhances its reactivity, particularly in the acidic region. In neutral and basic solution, the main reaction pathway for hydrolysis is *via* reaction of  $\text{HO}^-$  with the monoprotinated species for *N*-alkylformamidines and directly with the neutral species for *N*-arylformamidines. Unlike other simple formamidines studied to date, (7) also undergoes acid-catalysed hydrolysis, involving water

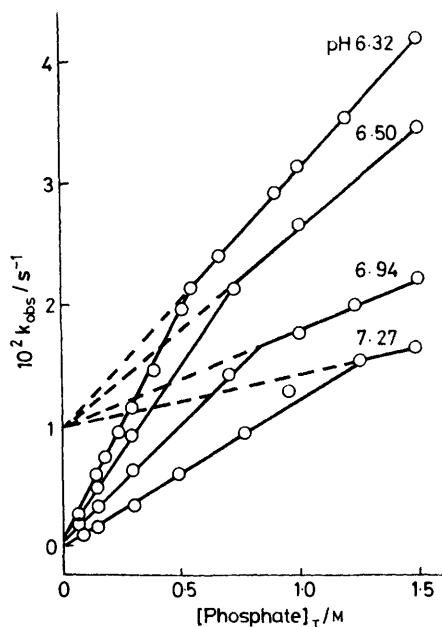


FIGURE 8 Observed rate constants ( $k_{\text{obs}}/\text{s}^{-1}$ ) for the hydrolysis of (7b) at 25° in water as a function of total phosphate buffer concentration

attack on the mono- and di-protonated substrate. Marked general acid catalysis of hydrolysis is observed in all cases and the non-linear buffer plots have been ascribed to a change in the rate-limiting step at high buffer concentration.

#### EXPERIMENTAL

***t*-Butyl Isocyanide.**—*t*-Butylformamide (20 g) was dissolved in pentane (44 ml) and pyridine (89.5 g) and cooled at 0–5°. Phosphoryl chloride (34.8 g) was added over 30 min and the solution was then heated at 60° for 15 min. On cooling, ice-water (200 ml) was added and the organic phase extracted (2 × 30 cm) with pentane. Evaporation of the pentane gave the isocyanide (60%), b.p. 93–95° (lit.,<sup>20</sup> 93–95°),  $\nu_{\text{max}}$  2 165  $\text{cm}^{-1}$  ( $\text{N}=\text{C}$ ).

**Phenyl Isocyanide.**—Triphenoxyphosphine (13.1 g) was added to phenyl isocyanide dichloride (8.7 g). The mixture was stirred and gradually heated to 60°; an exothermic reaction took place and the temperature rapidly rose to 100°. The dark brown residue obtained was distilled to give the isocyanide (48%), b.p. 54–55° at 0.9 mmHg (lit.,<sup>21</sup> 57–58 °C at 0.5 mmHg).

***p*-Nitrophenyl Isocyanide.**—Phosgene (6.0 g) was liquified at –70° and dissolved in methylene chloride (15 ml). The solution was added dropwise with stirring to a mixture of 4-nitrophenylformamide (8.5 g) and triethylamine (10.1 g)

in methylene chloride (200 ml). The solution gradually became homogeneous and stirring was continued for a further 2 h under nitrogen to remove traces of unchanged phosgene. The solvent was removed *in vacuo* and the residue taken up in pentane (80 ml). Concentration of the solution gave the isocyanide (65%), m.p. 119° (lit.,<sup>22</sup> 119–120°).

**1-(*N*-*t*-Butylformimidoyl)imidazole.**—Imidazole (7.0 g) was added to a solution of *t*-butyl isocyanide (8.3 g) in dry benzene (30 ml) containing finely powdered silver chloride (14.3 g) and the mixture was refluxed for 6 h. On removal of the silver chloride, distillation gave 1-(*N*-*t*-butylformimidoyl)imidazole, b.p. 96–97° at 0.08 mmHg (lit.,<sup>23</sup> 104° at 1 mmHg),  $\nu_{\text{max}}$  1 675  $\text{cm}^{-1}$  ( $\text{C}=\text{N}$ );  $\delta$  (neat) 1.3 (9 H, s), 7.08 (1 H, m), 7.48 (1 H, m), 7.95 (1 H, m), and 8.14 (1 H, s). Similarly prepared were 1-(*N*-phenylformimidoyl)imidazole (68%), b.p. 130° at 0.5 mmHg,  $\nu_{\text{max}}$  1 675  $\text{cm}^{-1}$  (Found: C, 70.2; H, 5.3; N, 24.5.  $\text{C}_{10}\text{H}_9\text{N}_3$  requires C, 70.3; H, 5.2; N, 24.7%) and 1-(*N*-*p*-nitrophenylformimidoyl)imidazole (70%), m.p. 120–122°,  $\nu_{\text{max}}$  1 675  $\text{cm}^{-1}$  (Found: C, 55.7; H, 3.5; N, 26.2.  $\text{C}_{10}\text{H}_8\text{N}_4\text{O}_2$  requires C, 55.5; H, 3.7; N, 25.9%).

1-(*N*-*t*-Butyl[<sup>2</sup>H]formimidoyl)imidazole was similarly prepared using imidazole which had been repeatedly recrystallised from  $\text{D}_2\text{O}$ . The benzene used as solvent was also shaken with  $\text{D}_2\text{O}$  before drying. N.m.r. indicated (signal at  $\delta$  8.20) 77% deuteration.

**1-(*N*-*t*-Butylformimidoyl)morpholine.**—A mixture of *t*-butyl isocyanide (2.78 g), morpholine (8.7 g), and copper(I) chloride (0.02 g) was refluxed for 1 h. Ether was added to extract the organic product; evaporation of the dried extracts gave the morpholine derivative on distillation, b.p. 40° at 0.1 mmHg,  $\nu_{\text{max}}$  1 675  $\text{cm}^{-1}$  (Found: C, 63.7; H, 10.2; N, 16.7.  $\text{C}_9\text{H}_{16}\text{N}_2\text{O}$  requires C, 63.5; H, 10.6; N, 16.45%).

***N*-Phenylacetimidoyl Chloride.**—Thionyl chloride (22.5 ml) was added to acetanilide (13.5 g) and the mixture was gently refluxed for 20 min while HCl was evolved. On cooling excess of thionyl chloride was removed *in vacuo* and the residue yielded the chloride (75%), m.p. 118–120°,  $\nu_{\text{max}}$  1 655  $\text{cm}^{-1}$ ,  $\delta(\text{CDCl}_3)$  2.48 (3 H, s), 7.35–7.8 (5 H, m) (Found: C, 62.5; H, 5.0; N, 8.95.  $\text{C}_8\text{H}_8\text{ClN}$  requires C, 62.7; H, 5.2; N, 9.1%).

**1-(*N*-Phenylacetimidoyl)imidazole.**—Equimolar quantities of imidazole (3.4 g) and dry triethylamine (5.05 g) were dissolved in benzene (50 ml) and *N*-phenylacetimidoyl chloride (7.65 g) was added. The resulting solution was refluxed for 5 h and then extracted with ether. Evaporation of the dried extracts gave the imidazole derivative (55%), m.p. 106–108°;  $\nu_{\text{max}}$  1 671  $\text{cm}^{-1}$ ;  $\delta(\text{CDCl}_3)$  2.18 (3 H, s), 7.18–7.75 (8 H, s) (Found: C, 70.3; H, 6.4; N, 22.5.  $\text{C}_{11}\text{H}_{11}\text{N}_3$  requires C, 71.4; H, 5.9; N, 22.7%).

**1-(*N*-Phenylbenzimidoyl)imidazole.**—Equimolar amounts of imidazole (3.4 g, 0.05 mol) and dry triethylamine (5.05 g, 0.05 mol) were dissolved in benzene (50 ml) and *N*-phenylbenzimidoyl chloride (5.4 g) was added. The solution was refluxed for 5 h, cooled, and filtered to remove the hydrochloride salt. The solvent was removed under reduced pressure and the residue was extracted into ether. On removal of the ether a pale yellow solid remained which was recrystallized from hexane, m.p. 106–108°;  $\nu_{\text{max}}$  1 630–1 665  $\text{cm}^{-1}$  (Found: C, 77.9; H, 5.4; N, 17.0.  $\text{C}_{16}\text{H}_{13}\text{N}_3$  requires C, 77.7; H, 5.2; N, 17.0%).

## REFERENCES

- <sup>1</sup> S. J. Benkovic, *Accounts Chem. Res.*, 1978, **11**, 314.
- <sup>2</sup> D. R. Robinson and W. P. Jencks, *J. Amer. Chem. Soc.*, 1967, **89**, 7088, 7089.
- <sup>3</sup> D. R. Robinson, *J. Amer. Chem. Soc.*, 1970, **92**, 3138.
- <sup>4</sup> P. A. Burdick, P. A. Benkovic, and S. J. Benkovic, *J. Amer. Chem. Soc.*, 1977, **99**, 5716.
- <sup>5</sup> U. K. Pandit and H. Bieraugel, *J.C.S. Chem. Comm.*, 1979, 117; R. A. Gase and U. K. Pandit, *ibid.*, 1977, 480.
- <sup>6</sup> R. H. DeWolfe, *J. Amer. Chem. Soc.*, 1960, **82**, 1585; 1964, **86**, 864.
- <sup>7</sup> R. H. DeWolfe in 'The Chemistry of Amidines,' ed. S. Patai, Wiley-Interscience, New York, p. 349.
- <sup>8</sup> H. A. Staab, *Angew. Chem. Internat. Edn.*, 1962, **1**, 351.
- <sup>9</sup> T. C. Bruice and G. L. Schmir, *J. Amer. Chem. Soc.*, 1957, **79**, 1663.
- <sup>10</sup> T. H. Fife, *J. Amer. Chem. Soc.*, 1965, **87**, 4597.
- <sup>11</sup> A. F. Hegarty, J. D. Cronin, and F. L. Scott, *J.C.S. Perkin II*, 1975, 429.
- <sup>12</sup> D. G. Oakenfull and W. P. Jencks, *J. Amer. Chem. Soc.*, 1971, **93**, 178.
- <sup>13</sup> R. B. Moodie and R. Towill, *J.C.S. Perkin II*, 1972, 184.
- <sup>14</sup> A. F. Hegarty, C. N. Hegarty, and F. L. Scott, *J.C.S. Perkin II*, 1974, 1258.
- <sup>15</sup> M. I. Page and W. P. Jencks, *J. Amer. Chem. Soc.*, 1972, **94**, 8828.
- <sup>16</sup> As judged from  $k_{\text{HO}^-}/k_{\text{H}_2\text{O}}$  rates for other reactions (see for example, W. P. Jencks and J. Carriuolo, *J. Amer. Chem. Soc.*, 1960, **82**, 1778; A. F. Hegarty, C. N. Hegarty, and F. L. Scott, *J.C.S. Perkin II*, 1975, 1167).
- <sup>17</sup> W. P. Jencks and J. Carriuolo, *J. Amer. Chem. Soc.*, 1961, **83**, 1743.
- <sup>18</sup> Hammett  $\rho$  values of this magnitude have been obtained for nucleophilic attack on imines (see Y. Ogata and A. Kawasaki, *J.C.S. Perkin II*, 1979, 720 and references therein).
- <sup>19</sup> E. N. Peters, *J. Amer. Chem. Soc.*, 1976, **98**, 5627; E. N. Peters and H. C. Brown, *ibid.*, 1975, **97**, 1712, 2892.
- <sup>20</sup> J. Casanova, N. D. Werner, and E. R. Schuster, *J. Org. Chem.*, 1966, **31**, 3473.
- <sup>21</sup> I. Ugi and R. Meyer, *Angew. Chem.*, 1958, **70**, 702.
- <sup>22</sup> H. Malz and E. Kuehle, *Chem. Abs.*, 1964, **60**, 6795.
- <sup>23</sup> Y. Ito, Y. Inubishi, and T. Saegusa, *Tetrahedron Letters*, 1974, 1283.